



Accepted Article

Title: Photocatalytic Phenol-Arene C-C and C-O Cross-Dehydrogenative Coupling

Authors: Anna Eisenhofer, Johnny Hioe, Ruth Gschwind, and Burkhard König

This manuscript has been accepted after peer review and appears as an Accepted Article online prior to editing, proofing, and formal publication of the final Version of Record (VoR). This work is currently citable by using the Digital Object Identifier (DOI) given below. The VoR will be published online in Early View as soon as possible and may be different to this Accepted Article as a result of editing. Readers should obtain the VoR from the journal website shown below when it is published to ensure accuracy of information. The authors are responsible for the content of this Accepted Article.

To be cited as: *Eur. J. Org. Chem.* 10.1002/ejoc.201700211

Link to VoR: <http://dx.doi.org/10.1002/ejoc.201700211>

Photocatalytic Phenol–Arene C–C and C–O Cross-Dehydrogenative Coupling

Anna Eisenhofer,^[a] Johnny Hioe,^[a] Ruth M. Gschwind,^{*[a]} and Burkhard König^{*[a]}

Abstract: Phenol-containing non-symmetrical biaryls play an important role in natural product synthesis, as ligands in metal catalysis and for organic functional materials. Cross-coupling reactions by twofold direct C–H activation for their synthesis are important and challenging transformations. In the last decade, a variety of useful oxidative methods have been developed. The key for efficiency and selectivity typically constitutes the application of highly fluorinated solvent systems. Herein, we describe the visible light-mediated C–C and C–O cross-coupling of electron-rich phenols and arenes by using Ru(bpz)₃(PF₆)₂ as photocatalyst and ammonium persulfate as terminal oxidant. The method requires no leaving group functionalities, which allows the use of simple activated arenes as starting materials. Furthermore, the approach features a good chemo- and regioselectivity as well as functional group tolerance even by replacement of fluoroalcohols by acetonitrile. The selectivity for the formation of the non-symmetrical biaryls is rationalized on basis of the nucleophilicity *N* values and oxidation potentials *E*_{ox} of the electron-rich substrates.

Introduction

Non-symmetrical biaryls including a phenol moiety represent an important structural motif in natural products and pharmaceutical active compounds,^[1] as phenols, especially oxygenated derivatives like guaiacol, are ubiquitous in nature and their oxidation is involved in the biogenesis of biologically active, naturally occurring products.^[2] Moreover, biaryls constitute important ligands for transition metal catalysis^[3] and are versatile building blocks for organic functional materials.^[4] Conventional C–C cross-coupling strategies for the synthesis of biaryls, like Suzuki and Negishi coupling, are powerful and established methods, but require the prefunctionalization of the starting materials by introduction of leaving groups, complex catalyst systems often based on transition metals and typically a protection of the phenol hydroxyl group.^[5] Due to the impact of green chemistry principles in organic synthesis the demand for the development of cross-coupling methods by direct C–H functionalization emerged. Over the past decades a variety of efficient protocols for the cross-coupling of arenes with only one prefunctionalized coupling partner were developed.^{[6],[7]} Especially attractive in terms of atom economy and efficiency is the cross-coupling of arenes by twofold direct C–H activation.^{[6c–e, 8],[9]} However, the absence of leaving functionalities constitutes

at the same time a severe challenge due to the possible formation of undesired homocoupling products, regioisomers and overoxidation products. Metal salts such as Cu^{II},^[10] Fe^{III},^[11] Ti^{IV},^[12] Al^{III},^[13] Mo^V,^[14] Tl^{III}^[15] have been successfully employed as stoichiometric oxidants for the formation of biaryls. Also combinations of metal catalysts (i.e. Pd, Fe, Cr, Cu) and a metal-free terminal oxidant (i.e. air) are reported.^[16] However, these transformations are often limited to the homocoupling of arenes or suffer from low chemoselectivity as well as (toxic) metal waste. The challenge is to identify the factors that determine the chemo- and regioselectivity and thus, to control the formation of the anticipated cross-coupling products.

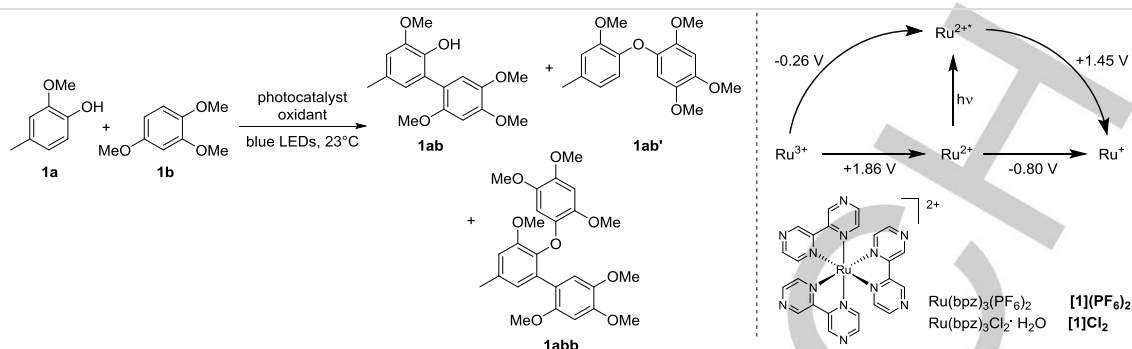
Recent developments in the field of oxidative phenol–arene C–C cross-coupling demonstrated the applicability of hypervalent-iodine based oxidants as reported by Kita *et al.*^[17], electrochemical methods as described by Waldvogel *et al.*^[18] and iron-catalyzed transformations using *t*-BuOO*t*-Bu as terminal oxidant published by Pappo *et al.*^[19] These strategies provided a selective and easy access to the respective cross-coupling products, but are typically limited in terms of efficiency and (chemo)selectivity to highly fluorinated solvent systems, in particular 1,1,1,3,3,3-hexafluoro-2-propanol (HFIP), which are expensive and have a large environmental footprint. Despite the possibility of recycling of HFIP as shown for the electrochemical protocol, the replacement of the fluorinated media would be highly desirable. Waldvogel *et al.* obtained promising results by substitution of HFIP by solvents with a strong hydrogen bonding capability, like formic acid. The C–C cross-coupling products were formed with good selectivity, but reduced yields.^[18c, 20]

Different rationales were developed in order to explain the observed efficiency and tendency for cross- vs. homocoupling. Waldvogel and coworker rationalized the selectivity for C–C cross-coupling as a result of a decoupling of oxidation potential *E*_{ox} and nucleophilicity by formation of different HFIP solvates.^[18d] Pappo *et al.* developed an operational simple tool to predict the selectivity for iron-catalyzed phenol–phenol C–C cross-coupling reactions, which proceed via a radical–anion coupling mechanism, by comparing the *E*_{ox} and nucleophilicity *N* values of the phenol substrates.^{[19b],[21]} On the basis of the model a selective C–C cross-coupling takes place if the phenol component **a** is more readily oxidized to the corresponding phenoxyl radical **a**[•] than the phenol coupling partner **b** (*E*_{ox}(**a**) < *E*_{ox}(**b**)), which constitutes the stronger nucleophile (*N*_b > *N*_a).

In the last decade, visible light photoredox catalysis developed as a mild and versatile method for the activation of C–H bonds and may provide a valuable, alternative mechanistic concept for the oxidative biaryl synthesis.^[22] The feasibility of phenol activation by photocatalysis was demonstrated by early work of Ohkubo *et al.*; they described the photocatalytic homodimerization of naphthols.^[23] Recent examples from the groups of Yoon and Wang photocatalytically activated phenols for the construction of dihydrobenzofurans.^[24] Rüping *et al.* developed a method for the *ortho* olefination of protected phenols bearing a directing group in a dual catalytic approach.^[25]

[a] Dr. A. Eisenhofer, Dr. J. Hioe, Prof. Dr. R. M. Gschwind, Prof. Dr. B. König
University of Regensburg, Faculty of Chemistry and Pharmacy,
Institute of Organic Chemistry, D-93040 Regensburg, Germany
E-mail: Ruth.Gschwind@ur.de, Burkhard.Koenig@ur.de
<http://www-oc.chemie.uni-regensburg.de/gschwind/>
<http://www-oc.chemie.uni-regensburg.de/koenig/>

Supporting information for this article is given via a link at the end of the document.

Table 1. Optimization of reaction conditions for the oxidative phenol–arene cross-coupling.^{[a],[b]}

Entry ^[a]	Equiv. 1b	Catalyst	Solvent	t [h]	Oxidant	Conv. 1a % ^[c]	Yield [%] ^[c]		
							1ab	1ab'	1abb
1	3	2 mol% [1](PF ₆) ₂	HFIP/MeOH ^[d]	24	Air	43	30	3	-
2	3	2 mol% [1]Cl ₂	HFIP/MeOH ^[d]	24	Air	68	48	5	2
3	3	2 mol% [1](PF ₆) ₂	MeCN	24	Air	73	52	4	1
4	3	2 mol% [1](PF ₆) ₂	MeCN	36	Air	79	53	3	2
5	3	4 mol% [1](PF ₆) ₂	MeCN	24	Air	81	50	2	1
6	3	2 mol% [1](PF ₆) ₂	MeCN	24	(NH ₄) ₂ S ₂ O ₈	96	65	7	23
7	3	2 mol% [1](PF ₆) ₂	MeCN	18	(NH ₄) ₂ S ₂ O ₈	96	66	7	24
8	2	2 mol% [1](PF ₆) ₂	MeCN	18	(NH ₄) ₂ S ₂ O ₈	96	66	5	19
9	1.5	2 mol% [1](PF ₆) ₂	MeCN	18	(NH ₄) ₂ S ₂ O ₈	96	59	4	18
10	1	2 mol% [1](PF ₆) ₂	MeCN	18	(NH ₄) ₂ S ₂ O ₈	87	37	8	8
11	2	1 mol% [1](PF ₆) ₂	MeCN	18	(NH ₄) ₂ S ₂ O ₈	97	68	5	26
12	2	0.5 mol% [1](PF ₆) ₂	MeCN	18	(NH ₄) ₂ S ₂ O ₈	97	69 (62)	5 (5)	23 (23)
13	3	2 mol% [1](PF ₆) ₂ ^[e]	MeCN	18	(NH ₄) ₂ S ₂ O ₈	-	0	0	-
14	2	No catalyst	MeCN	18	(NH ₄) ₂ S ₂ O ₈	13	3	0	-

[a] Reaction conditions: 2-methoxy-4-methylphenol **1a** (0.20 mmol, 0.25 M), 1,2,4-trimethoxybenzene **1b** (1–3 equiv.), air or ammonium persulfate (1.5 equiv.) and the respective photocatalyst were irradiated with blue LEDs open to air for entries 1–5 and under a N₂-atmosphere for entries 6–14 at 23 °C in the respective solvent (dry), unless otherwise noted. [b] The potentials of the catalyst are given in Volt vs. SCE.^[26] [c] Quantitative HPLC yields using acetanilide as internal standard. [d] HFIP + 18 Vol% MeOH. [e] Reaction under exclusion of light.

The visible light-mediated amination of phenols^[27] and arenes^[28] was reported recently.

In this study, a visible light-mediated oxidative phenol–arene cross-coupling reaction is described using Ru(bpz)₃(PF₆)₂ as photocatalyst with low catalyst loadings and ammonium persulfate as mild terminal oxidant. The approach requires no leaving group functionalities or protection of the phenol hydroxyl group, which allows the use of simple electron-rich starting materials. The observed selectivity is rationalized by comparing the oxidation potential *E*_{ox} and nucleophilicity *N* values of the substrates.

Results and Discussion

We focused our initial studies on the oxidative cross-coupling between 4-methylguaiacol **1a** and 1,2,4-trimethoxybenzene **1b**, which are reported to undergo preferentially cross- instead of homocoupling by electrochemical oxidation in HFIP/MeOH solvent systems,^[18b] to find and optimize suitable photocatalytic conditions. The photoreactions were performed at 23 °C and irradiated with blue LEDs. Ru(bpz)₃(PF₆)₂ [**1**] was used as photocatalyst, as phenols are literature known reductive quencher of its excited state (Table 1).^[29] To our delight, when air was used as terminal oxidant, the desired cross-coupling

product **1ab** was obtained in 30% yield along with traces of the C–O connected cross-coupling product **1ab'** (Table 1, entry 1). Such bis-aryl ether by-products for the oxidative cross-coupling of phenols and arenes are rare and are reported by the groups of Peddinti^[30] and Waldvogel^[18b] for very few examples. The exchange of the counterion from PF₆⁻ to Cl⁻ improved the solubility of the photocatalyst in the HFIP/MeOH mixture and led to an increased product yield of 48% (Table 1, entry 2). A screen of solvents showed that acetonitrile could substitute the highly fluorinated solvent mixture without loss of selectivity and even a slightly increased yield (Table 1, entries 1–3 and Table S1 in the SI). In acetonitrile an exchange of the counterion to chloride was detrimental (for details see SI). An enhanced reaction time or catalyst loading could not further improve the yield, but the replacement of air by ammonium persulfate as terminal oxidant led to full conversion of the activated phenol **1a** (Table 1, entries 4–6) and the non-symmetrical biaryl **1ab** was obtained in 65% yield. Ammonium persulfate is a reported oxidative quencher of photoexcited ruthenium polypyridyl complexes and provide access to the strongly oxidative Ru(bpz)₃³⁺ species for the phenol oxidation.^[31] The combination of Ru(bpz)₃(PF₆)₂ and persulfate was also beneficial for the [3+2]-cycloaddition of activated phenols and styrenes reported by Yoon *et al.*^[24a] The C–C vs C–O chemoselectivity for the biaryl products (**1ab:1ab'**) almost retained under these conditions. However, the stronger

oxidative conditions led to a higher formation of the teraryl **1abb** as a single isomer. Within the system with ammonium persulfate as terminal oxidant the equivalents of the electron-rich coupling partner **1b** and the catalyst loading could be reduced without loss of selectivity and yield (Table 1, entries 7-10, 11-12). A change of the photocatalyst to the less oxidizing Ru(bpy)₃(PF₆)₂ [**2**] results in slower rates and incomplete conversion (Table S2 in the SI). The homocoupling product **1bb** was not detected by HPLC under all applied conditions (< 1% with regard to the detection limit). Control experiments in the absence of photocatalyst or light confirmed the photocatalytic nature of the reaction (Table 1, entries 13-14).^[32]

The scope of the oxidative phenol–arene cross-coupling was investigated using the optimized reaction conditions (phenol (1 equiv., 0.25 M in MeCN (dry), arene (2 equiv.), ammonium persulfate (1.5 equiv.) and Ru(bpz)₃(PF₆)₂ (0.5–2 mol%), blue LEDs, N₂, 23 °C). The results are summarized in Table 2.

The desired C–C cross-coupled biaryls **ab** were obtained for various combinations of electron-rich phenols and arenes with moderate to good yields and high functional group tolerance. To our surprise a varying content of C–O connected biaryls **ab'** were isolated, which even became the main product for some phenol–arene pairs.^[33]

In order to explain the observed product distribution for the biaryl formation (coupling mode and cross- vs. homocoupling), the oxidation potentials E_{ox} and nucleophilicity N values^{[34],[35]} of the electron-rich substrates were determined by cyclic voltammetry (CV) and density functional theory (DFT) methods (Table 3), respectively, and analyzed in analogy to the electrochemical^[18d] and iron-catalyzed^[19b] selectivity rationales for oxidative cross-coupling reactions.

The first selectivity determining parameter for the formation of the biaryl products is the initiating oxidation step. Depending on the tendency for oxidation, which can be estimated from E_{ox} , either the phenol **a** or the arene **b** are assumed to enter the catalytic cycle and provide the corresponding phenoxy radical **a'** (pathway 1: $E_{ox}(a) < E_{ox}(b)$) or arene radical cation **b''** (pathway 2: $E_{ox}(a) > E_{ox}(b)$) (Scheme 1). Phenoxy radicals **a'** are resonance-stabilized and the spin density distribution depends amongst others on the type and position of the substituents. However, phenoxy radicals **a'** with unsubstituted *ortho*- or *para*-positions are reputed to couple via these electrophilic carbon atoms in the first coupling step.^{[18b],[33],[36],[37],[38]} The second parameter, which we propose to determine the efficiency and selectivity in analogy to the literature reported rationales,^[18d, 19b] is the nucleophilicity strength N of the coupling partner.

On the basis of our results we propose, that the C–C coupled biaryls **ab** are formed predominately on the pathway 1 via the intermediacy of the phenoxy radicals **a'**, which are trapped by an arene nucleophile **b**, if **b** provides a high N value. Whereas, the C–O coupled biaryls **ab'** are assumed to be accessed via the pathway 2 with the phenol component **a** acting predominately as *O*-nucleophile trapping the arene radical cation **b''**. The formation of the homocoupling products **bb** is proposed to proceed via pathway 2. The final products are obtained after another oxidation/deprotonation step (Scheme 1).

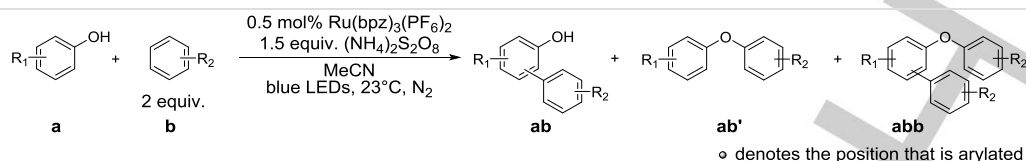
Under consideration of the E_{ox} and N values, the phenol–arene pairs were divided in 3 categories (Table 2). In categories 1-2 the oxidation of the phenol **a** is thermodynamically favored ($E_{ox}(a) < E_{ox}(b)$) and the nucleophilicity N of the arene coupling partner **b** range from strong (category 1) to moderate (category 2). Category 3 covers the inverse region of the oxidation potentials ($E_{ox}(a) > E_{ox}(b)$) in the presence of the strong, electron-rich arene nucleophile **1b**.

Table 3. Oxidation potentials E_{ox} and calculated global nucleophilicity N values of various activated phenols and arenes. The oxidation potentials are sorted in an increasing order.

Entry	Substrate	E_{ox} [V] ^[a]	N (eV) ^[b]
1	4-methoxy-1-naphthol (2a)	0.87	4.05
2	1,2,4-trimethoxybenzene (1b)	1.01	4.07
3	2-tert-butyl-4-methoxyphenol (4a)	1.02	3.81
4	4-methoxy-2-methylphenol (3a)	1.02	3.82
5	2,6-dimethoxyphenol (5a)	1.10	3.64
6	2-methoxy-4-methyl-phenol (1a)	1.10	3.68
7	4-ethyl-2-methoxyphenol (6a)	1.11	3.70
8	4-allyl-2-methoxyphenol (7a)	1.15	3.63
9	4-chloro-2-methoxy-phenol (8a)	1.23	3.37
10	2-chloro-4-methylphenol (9a)	1.32	3.09
11	1,3,5-trimethoxybenzene (3b)	1.34	3.55
12	2,6-diphenylphenol (10a)	1.35	3.38
13	2-methoxynaphthalene (2b)	1.36	3.51
14	1-bromo-2,4-dimethoxybenzene (4b)	1.48	3.46

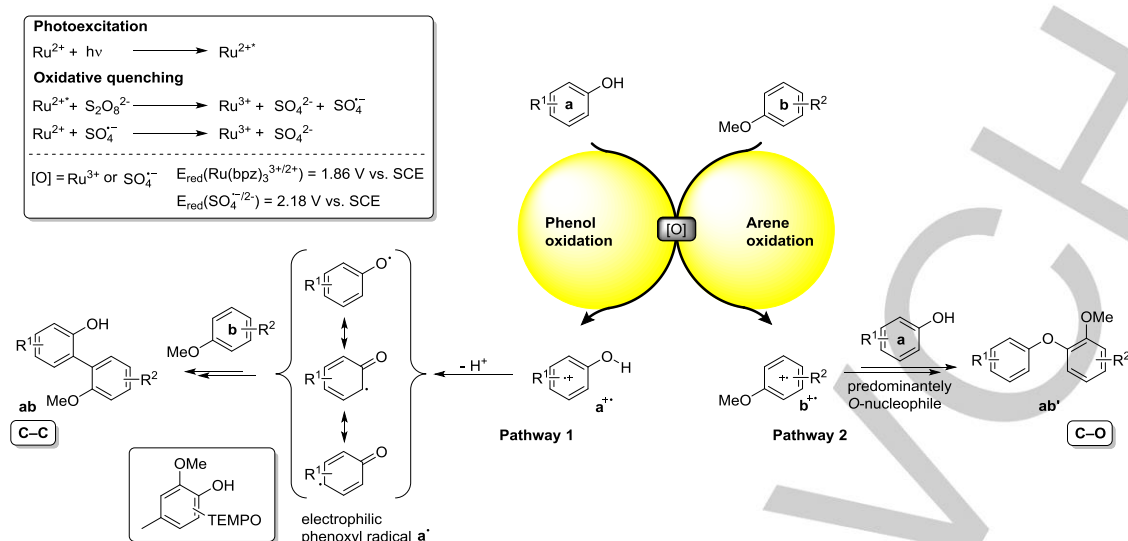
^[a] The oxidation potentials (peak potentials) were determined by CV using tetrabutylammonium tetrafluoroborate as the supporting electrolyte in MeCN (0.1 M) at a scan rate of 50 mV s⁻¹. Ferrocene was used as internal standard. The potentials are given in Volt vs. SCE.^[39] ^[b] The energy of the HOMO of the selected substrate was calculated by DFT methods at the B3LYP-D3/6-311+G(d,p) level of theory^[35] and the nucleophilicity N values are referenced against the HOMO of tetracyanoethylene (TCE).

Category 1 ($E_{ox}(a) \leq E_{ox}(b)$, $N_b \geq N_a$). For phenol–arene pairs of category 1 the oxidation of the phenol component (**2a-4a**) is favored and the arene coupling partner **1b** constitutes a strong nucleophile, which is shown by a high N value (4.07 eV). The expected biaryl C–C cross-coupling products (**2ab-4ab**) are obtained with moderate to good yields and selectivity. The arene **1b** reacted at the most nucleophilic position and no regioisomers as well as homocoupling products or C–O coupled biaryls **ab'** were formed supporting the mechanistic rationale in Scheme 1. Interestingly, for 4-alkoxy cross-coupling products (**2ab-4ab**) a prolonged irradiation time and higher catalyst loading led to a further oxidation to the corresponding benzo- and naphthoquinone products (**2q-4q**) (see Scheme 2).^[40] The profile (see Figure S13 in the SI) of the reaction between 4-methoxy-1-naphthol **2a** and 1,2,4-trimethoxybenzene **1b** indicates that the formation of the products takes place successively and excludes the formation of the naphthoquinone product **2q** by cross-coupling of oxidized naphthol starting material with arene **1b**. Using 2 mol% Ru(bpz)₃(PF₆)₂ under otherwise identical conditions provided 67% **2q** after 18 h of irradiation with blue LEDs.

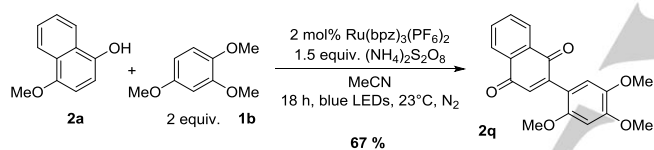
Table 2. Scope of the photocatalytic oxidative phenol–arene cross-coupling by direct C–H activation. The phenols **a** are sorted in an increasing order regarding the oxidation potentials E_{ox} .^[a]

Category	Entry	Phenol	Arene	t [h] ^[b]	Yield [%] ^[c]				
					a _{recov.}	ab	ab'	abb	bb
1	1			3	5	78 (2ab)	-	- ^[e]	-
	2			5	24	61 (3ab)	-	- ^[f]	-
	3			6	41	44 (4ab)	-	- ^[g]	-
2	4			22	22	31 (5ab)	-	traces ^[j]	- ^{[i],[k]}
	5 ^[d]			16	-	24 (6ab)	traces ^[j]	traces ^{[i],[k]}	-
	6 ^[d]			18	10	23 (7ab)	-	30 (7abb)	-
	7 ^[d]			18	44	traces ^[j] (8ab)	-	-	- ^{[i],[k]}
3	8 ^[d]			18	-	79 (9ab)	-	15 (9abb)	-
	9			18	-	62 (1ab)	5 (1ab')	23 (1abb)	-
	10			18	5	46 (10ab)	6 (10ab')	24 (10abb)	-
	11			16	10	36 (11ab)	21 (11ab')	18 (11abb)	-
	12			21	27	21 (12ab)	34 (12ab')	10 (12abb)	4 (1bb)
	13			18	52	7 (13ab)	17 ^[j] (13ab')	traces ^{[i],[k]}	25 (1bb)
	14			40	19	10 (14ab)	44 (14ab')	27 (14abb)	6 (1bb)

[a] Reaction conditions: phenol (0.20 mmol, 0.25 M), arene (2 equiv.), ammonium persulfate (1.5 equiv.) and 0.5 mol% Ru(bpz)₃(PF₆)₂ were irradiated with blue LEDs under a N₂-atmosphere at 23 °C in MeCN (dry), unless otherwise noted. [b] End of reaction was judged by TLC and/or HPLC analysis indicated by either no further conversion of starting material or complete consumption of starting material. For 4-methoxyphenols and -naphthols a color change to dark red indicates initiation of quinone formation and marks the end of the reaction. [c] Yield of isolated products. [d] 2 mol% Ru(bpz)₃(PF₆)₂ were used. [e] 6% of naphthoquinone **2q** were isolated. [f] 5% of benzoquinone **3q** were isolated. [g] 15% of benzoquinone **4q** were isolated. [h] Local nucleophilicity index (N_k) values from reference^[34]. [i] A second minor regioisomer was detected. [j] The product amount was too small for preparative isolation and characterization. See LC-MS data in the Supporting Information. [k] Several teraryls as a mixture. [l] Traces of the homocoupling product of phenol **a** were detected by mass analytics.



Scheme 1. Proposed predominant pathways for the photocatalytic phenol–arene C–C and C–O oxidative cross-coupling reaction for the formation of biaryls **ab** and **ab'**.^{[41], [26a], [42]} Ammonium persulfate oxidatively quenches the excited state of $Ru(bpz)_3^{2+}$ generating the corresponding Ru^{3+} species and the oxygen-centered sulfate radical anion $SO_4^{\cdot-}$, which is a very strong oxidant capable of oxidizing Ru^{2+} in the ground state providing a second equivalent of Ru^{3+} .^{[31], [43]} The intermediacy of phenoxyl radicals was confirmed for the phenol–arene coupling between **1a** and **1b** by trapping with the persistent radical TEMPO.



Scheme 2. Photocatalytic formation of naphthoquinone–arene coupling product **2q**.

Category 2 ($E_{ox}(a) < E_{ox}(b)$, $N_b \approx N_a$). Category 2 covers phenol–arene pairs, for which the oxidation potential of the phenol **a** is significantly lower than for the arene **b**, but the nucleophilicity N values of both substrates are moderate and in the same range. On basis of the mechanistic rationale a mixture between the desired mixed C–C coupled biaryl **ab** and the homocoupling product of the corresponding phenol **aa** is expected. The mixed C–C coupled biaryls **5ab–7ab** were obtained with moderate yields. The nucleophilicity of arene **4b** is not sufficient to provide the respective cross-coupling product, determining the limit of the method. However, no phenol homocoupling products **aa** were isolated^[44] and the mass balance for the component **a** indicate, that the phenol components **a** undergo under these conditions polymerization rather than the expected dimerization. The absence of C–O coupled biaryls **5ab'**, **7ab'** and **8ab'** in category 2 further supports the mechanism proposed in Scheme 1 for their formation.

Category 3 ($E_{ox}(a) > E_{ox}(b)$, $N_b > N_a$). Phenols (**1a**, **5a–10a**) of category 3 exhibit a higher oxidation potential than the arene component **b**. The oxidation potentials of the phenolic substrate were increased stepwise from entry 8 to 14. Throughout the

investigated series within category 3 the arene **1b** was kept unchanged as strong nucleophile. According to the mechanistic rationale (Scheme 1) the formation of products derived from pathway 2, the C–O coupled product **ab'** and the homocoupling product **1bb** of the arene component, are expected. However, also the phenol–arene C–C cross-coupled biaryls (**1ab**, **9ab–14ab**) were formed with up to 79 % yield (**9ab**). Within the category 3 the amount of C–C coupled biaryl **ab** decreased with increasing oxidation potentials of the phenol **a** and thus, increasing off-set in the oxidation potentials between phenol **a** and arene **b**. The formation of the C–O coupled biaryl **ab'** initiates at an off-set in the potentials of $\sim 0.1 \text{ V}$, the arene homocoupling product **1bb** at an off-set of $\sim 0.2 \text{ V}$. Furthermore, the amount of **ab'** and **bb** increased as expected with the oxidation potential of the phenol substrate **a**.

Wenger *et al.* suggested that phenols can form weakly hydrogen bonded encounter adducts with the peripheral nitrogen atoms of the bipyrazine ligand of the $Ru(bpz)_3^{2+}$ catalyst.^[29] Furthermore, it is known that bases, e.g. pyridine or inorganic salts, lower the oxidation potential of phenolic compounds due to a partial deprotonation of the hydroxyl group resulting in an enhanced electron density and a facilitated electron transfer.^[45] Thus, we propose that a pre-organization between the phenol substrates **a** and the catalyst via hydrogen bonding occurs (not applicable for compound class **b**). We assume further that the pre-organization enables the selective and efficient conversion of substrates to the C–C cross-coupled biaryls **ab** via pathway 1 with an offset of $\Delta E_{ox} = E_{ox}(a) - E_{ox}(b) < 0.10 \text{ V}$. A similar effect was reported by Waldvogel and coworkers,^[18b] they showed that the addition of MeOH to the HFIP solvent reduced the oxidation potential of the phenol substrate, which allow the selective cross-coupling with arenes even if the original potential in pure HFIP was higher.

The mechanism in Scheme 1 for the formation of C–O coupled biaryls **ab'** via an O-nucleophilic attack of the phenol on the arene radical cation **b⁺** (pathway 2) is supported by comparing the relative amount of C–O coupled biaryls **ab'** and the homocoupling product **1bb** with the *N* values of the applied phenols **a**.^[46] Phenols with high nucleophilicity *N* value (**1a**, **6a-7a**) exclusively provided the biaryl **ab'** and no homocoupling product **1bb** is formed, phenols (**8a**, **10a**) with moderate *N* value led to a low formation of the symmetrical biaryl **1bb** in addition to the biaryl **ab'**, whereas for the very poorly nucleophilic phenol **9a** 25% of the by-product **1bb** were isolated. However, we also want to point out that the distribution of the spin density of phenoxy radicals **a[•]** is affected by the type and position of substituents on the aromatic ring, which can lead to an increased spin density on the O-atom and thus can serve as an alternative explanation for the formation of the C–O cross-coupled biaryls **ab'** by a cross-coupling of electrophilic **a[•]** with a nucleophile **b** via pathway 1.^[36a-e, 36g, 37a, 38] For example, bulky *ortho*-groups stabilize the O-radical and thus an increased reactivity of the phenoxy radical via the oxygen atom is possible.^[36g] Pappo *et al.* investigated the influence of *ortho*-groups on the regioselectivity and coupling mode for the consecutive formation of teraryls.^[36d] However, due to the dependency of the product distribution **ab':bb** on the nucleophilicity *N* of the phenol **a**, the correlation between the E_{ox} of the phenols **a** and the relative amount of C–O coupling product **ab'** as well as the high potential difference for category 3 couplings (in particular entries 12-14), we assume that the proposed mechanism in scheme 1 is dominant. A coexistence of both mechanisms cannot be unambiguously excluded at this stage.

In addition to the discussed biaryls the corresponding teraryls (**1abb**, **7abb**, **9abb-12abb**, **14abb**) were obtained in most cases as single isomeric species in minor amounts (Table 2).^[47] Overoxidation e.g. to oligomers or polymers constitutes a severe challenge especially for the cross-dehydrogenative coupling of oxygenated aryl compounds, because the products often exhibit a lower oxidation potential than the corresponding starting materials (compare Table S3 and Table S4 in the SI). For the electrochemical protocol the formation of undefined oligomeric and polymeric by-products is reported in some cases.^[18a] We observed a single teraryl species **abb**, which provide access to complex structures within a single step.^[48] In order to determine the pathways for the formation of the teraryl **1abb**, the biaryl products (**1ab**, **1ab'**) were isolated and subjected to the photocatalytic conditions (Figure S7 and Scheme S3 in SI). Both, the C–C **1ab** and C–O **1ab'** cross-coupling product provided the teraryl **1abb**. Thus, for the formation of teraryl species different pathways are possible. Consequently, the rationalization on basis of E_{ox} and *N* is not trivial and required further investigation. The possible formation routes are presented in the SI.

Within the constraints of $\Delta E_{ox} < 0.10$ V the efficiency and selectivity of the phenol–arene C–C cross-coupling for the formation of biaryls is competitive with previously reported systems under consideration of the replacement of HFIP. The C–O coupling, initiating at an off-set in the potentials of ~ 0.1 V, enables the formation of the bis-aryl ethers **ab'** without pre-

functionalization of the electron-rich substrates under mild, photocatalytic conditions. The access in a single step is very attractive and may constitute an alternative to conventional synthetic methods.^[49] However, further investigations are required to improve the efficiency and selectivity for the C–O coupling.

Conclusions

In conclusion, an efficient and mild photocatalytic C–C and C–O cross-dehydrogenative coupling of electron-rich phenols and arenes in a single step under visible light irradiation was reported, using low catalyst loadings of Ru(bpz)₃(PF₆)₂ and ammonium persulfate as terminal oxidant. The direct C–H activation avoids the pre-functionalization of the electron-rich starting materials and thus enables the use of simple arenes. Furthermore, the photocatalytic cross-coupling method has a high functional group tolerance (e.g. halogen-moieties are conserved) and provides good synthetic yields. The tendency and efficiency for cross- vs. homocoupling and the coupling mode were rationalized on basis of the oxidation potentials E_{ox} and nucleophilicity *N* values.

Experimental Section

General: NMR-spectra were recorded on a Bruker Avance 400 (III HD) (¹H: 400 MHz, ¹³C: 101 MHz; T = 300 K, if not stated otherwise), Bruker Avance 300 (¹H: 300 MHz, ¹³C: 75 MHz, T = 295 K) or a Bruker III 600 (¹H: 600 MHz, ¹³C: 151 MHz, T = 295 K) using the solvent residual peak as internal reference (CDCl₃: δ H 7.26; δ C 77.0). Chemical shifts δ are reported in ppm. Multiplicities are indicated, s (singlet), d (doublet), t (triplet), q (quartet), quint (quintet), sept (septet), m (multiplet); coupling constants (*J*) are given in Hertz (Hz). Reactions were monitored by thin-layer chromatography using silica gel plates ALUGRAM Xtra SIL G/UV254 from Macherey-Nagel; visualization was accomplished with UV light (254 nm or 366 nm). Flash column chromatography was performed on a Biotage Isolera One automated flash purification system with UV-Vis detector using Sigma Aldrich MN silica gel 60 M (0.040-0.063 mm, 230-400 mesh) for normal phase chromatography. Cyclic voltammetry (CV) measurements were performed with the three-electrode potentiostat galvanostat PGSTAT302N from Metrohm Autolab. Mass spectra were recorded on Finnigan MAT95 (EI-MS), Agilent Q-TOF 6540 UHD (ESI-MS, APCI-MS), Finnigan MAT SSQ 710 A (EI-MS, CI-MS) or ThermoQuest Finnigan TSQ 7000 (ES-MS, APCI-MS) spectrometer. HPLC analytics were performed on a HPLC 1220 from Agilent technologies fitted with a C18 analytical column (Phenomenex Luna, particle size 3 μ m, 150 x 2.0 mm, 100 Å) and VWD. HPLC was calibrated by the internal standard method (multi-level calibration, internal standard: acetanilide). Gradient elution was done with water (millipore, 0.05 v/v% trifluoroacetic acid) (solvent A) and acetonitrile (solvent B) at a constant flow rate of 0.3 mL/min. A gradient profile with the following proportions of solvent B was applied [t (min), % B]: (0, 10), (25, 90), (30, 90). The injection volume was 1 μ L. Column oven temperature was set to 40°C. The chromatograms were monitored with wavelength switching [t (min), λ (nm)]: (0, 260), (10, 280). For irradiation with blue light Osram Oslon SSL 80 LEDs (λ_{peak} = 440 nm, royal blue, operated at 700 mA) were used.

General procedure for the photocatalytic phenol-arene coupling: In a crimp cap vial the appropriate phenol (1.0 equiv., 200 μ mol),

Ru(bpz)₃(PF₆)₂ (0.5 - 2 mol %, see Table 2), ammonium persulfate (1.5 equiv.) and the arene coupling partner (2 equiv.) were dissolved in dry MeCN (0.25 M) equipped with a magnetic stir bar. The solution was degassed by three freeze-pump-thaw cycles. The resulting mixture was irradiated (blue LEDs) through the vial's plane bottom side for the indicated time. The temperature was kept constant at 23 °C. After the irradiation period the reaction mixture was diluted with EtOAc and filtered over a plug of silica gel. The filtrate was concentrated in vacuum and purified by automated flash column chromatography (silica gel, hexane/EtOAc).

2-Hydroxy-2',3,4',5'-tetramethoxy-5-methylbiphenyl (1ab):^[18a] ¹H NMR (300 MHz, CDCl₃): δ = 6.85 (s, 1H), 6.71 (d, *J* = 1.9 Hz, 1H), 6.69 (d, *J* = 1.9 Hz, 1H), 6.65 (s, 1H), 5.98 (s, 1H), 3.94 (s, 3H), 3.91 (s, 3H), 3.86 (s, 3H), 3.81 (s, 3H), 2.33 (s, 3H). ¹³C NMR (75 MHz, CDCl₃): δ = 150.25, 149.17, 147.34, 143.48, 140.79, 129.13, 125.10, 123.30, 118.47, 114.92, 111.13, 98.34, 57.17, 56.35, 56.03, 55.89, 21.05. MS (EI): *m/z* (%): 304.2 (100), 289.1 (17), 272.1 (5), 261.1 (11), 257.2 (34), 229.0 (7), 152.1 (12), 115.1 (7).

1,2,4-Trimethoxy-5-(2-methoxy-4-methylphenoxy)benzene (1ab'): *R*_f = 0.31 (hexane/EtOAc, 3:1). ¹H NMR (400 MHz, CDCl₃): δ = 6.78 (d, *J* = 1.8 Hz, 1H), 6.64 (s, 1H), 6.63 – 6.60 (m, 1H), 6.59 (s, 1H), 6.56 (d, *J* = 8.1 Hz, 1H), 3.89 (s, 6H), 3.80 (s, 3H), 3.73 (s, 3H), 2.31 (s, 3H). ¹³C NMR (101 MHz, CDCl₃): δ = 149.30, 145.56, 145.07, 144.92, 143.34, 138.41, 132.50, 120.89, 116.29, 113.27, 106.29, 100.48, 57.39, 56.52, 55.93, 21.10. HRMS (ESI): calcd. for C₁₇H₂₁O₅ (M+H)⁺, *m/z* = 305.1384; found 305.1387.

2',3,4',5'-Tetramethoxy-5-methyl-2-(2,4,5-trimethoxyphenoxy)-1,1'-biphenyl (1abb): *R*_f = 0.32 (hexane/EtOAc, 1:1). ¹H NMR (400 MHz, CDCl₃): δ = 6.77 (s, 1H), 6.77–6.73 (m, 2H), 6.44 (s, 1H), 6.41 (s, 1H), 6.19 (s, 1H), 3.83 (s, 3H), 3.77 (s, 3H), 3.76 (s, 3H), 3.70 (s, 3H), 3.68 (s, 3H), 3.61 (s, 3H), 3.60 (s, 3H), 2.37 (s, 3H). ¹³C NMR (101 MHz, CDCl₃): δ = 152.21, 150.69, 148.59, 142.92, 142.72, 142.27, 142.16, 141.95, 139.31, 134.15, 132.50, 124.34, 117.87, 114.66, 112.24, 101.46, 100.91, 97.33, 57.38, 56.62, 56.58, 56.21, 56.03, 55.93, 55.85, 21.46. HRMS (ESI): calcd. for C₂₆H₃₁O₈ (M+H)⁺, *m/z* = 471.2013; found 471.2011.

1-Hydroxy-4-methoxy-2-(2,4,5-trimethoxyphenyl)naphthalene (2ab):^[17b] ¹H NMR (300 MHz, CDCl₃): δ = 8.39 – 8.32 (m, 1H), 8.26 – 8.19 (m, 1H), 7.59 – 7.47 (m, 2H), 6.97 (s, 1H), 6.73 (s, 1H), 6.72 (s, 1H), 6.70 (s, 1H), 4.00 (s, 3H), 3.97 (s, 3H), 3.90 (s, 3H), 3.86 (s, 3H). ¹³C NMR (75 MHz, CDCl₃): δ = 149.64, 149.59, 149.45, 144.56, 142.82, 126.53, 126.04, 125.88, 125.67, 122.75, 121.52, 119.53, 117.97, 115.37, 106.42, 98.96, 57.87, 56.61, 56.20, 55.82. MS (ESI): *m/z* (%) = 341.1 (43, MH⁺), 703.3 (21, 2MNa⁺).

2-(2,4,5-Trimethoxyphenyl)naphthalene-1,4-dione (2q):^[50] ¹H NMR (600 MHz, CDCl₃): δ = 8.17 – 8.09 (m, 2H), 7.78 – 7.73 (m, 2H), 7.05 (s, 1H), 6.83 (s, 1H), 6.62 (s, 1H), 3.95 (s, 3H), 3.86 (s, 3H), 3.78 (s, 3H). ¹³C NMR (151 MHz, CDCl₃): δ = 185.32, 183.93, 152.27, 151.27, 147.31, 143.09, 136.46, 133.64, 133.53, 132.70, 132.15, 126.94, 125.92, 114.27, 114.19, 97.72, 56.64, 56.60, 56.12. MS (ESI): *m/z* (%) = 325.1 (100, MH⁺), 671.2 (28, 2MNa⁺).

2-Hydroxy-2',5,4',5'-tetramethoxy-3-methylbiphenyl (3ab): *R*_f = 0.23 (hexane/EtOAc, 3:1). ¹H NMR (400 MHz, CDCl₃): δ = 6.85 (s, 1H), 6.75 (d, *J* = 2.9 Hz, 1H), 6.66 (s, 1H), 6.66 (d, *J* = 2.5 Hz, 1H), 6.09 (s, 1H), 3.95 (s, 3H), 3.86 (s, 3H), 3.84 (s, 3H), 3.79 (s, 3H), 2.32 (s, 3H). ¹³C NMR (101 MHz, CDCl₃): δ = 153.05, 149.62, 149.54, 145.82, 144.29, 127.35, 126.19, 118.94, 115.77, 115.26, 113.47, 98.47, 57.53, 56.47,

56.19, 55.70, 16.87. HRMS (ESI): calcd. for C₁₇H₂₁O₅ (M+H)⁺, *m/z* = 305.1384; found 305.1387.

2',4',5'-Trimethoxy-3-methyl-[1,1'-biphenyl]-2,5-dione (3q): *R*_f = 0.22 (hexane/EtOAc, 3:1). ¹H NMR (300 MHz, CDCl₃): δ = 6.76 (d, *J* = 2.7 Hz, 1H), 6.72 (s, 1H), 6.63 (dq, *J* = 3.0, 1.6 Hz, 1H), 6.58 (s, 1H), 3.93 (s, 3H), 3.84 (s, 3H), 3.76 (s, 3H), 2.11 (d, *J* = 1.6 Hz, 3H). ¹³C NMR (75 MHz, CDCl₃): δ = 187.84, 186.40, 152.04, 151.12, 146.28, 145.30, 142.99, 133.99, 132.98, 113.93, 97.55, 56.57, 56.52, 56.07, 16.41. HRMS (ESI): calcd. for C₁₆H₁₇O₅ (M+H)⁺, *m/z* = 289.1071; found 289.1076.

3-(tert-Butyl)-2-hydroxy-2',5,4',5'-tetramethoxy-biphenyl (4ab):^[17d] *R*_f = 0.33 (hexane/EtOAc, 3:1). ¹H NMR (300 MHz, CDCl₃): δ = 6.93 (d, *J* = 3.1 Hz, 1H), 6.86 (s, 1H), 6.67 – 6.64 (m, 2H), 6.09 (s, 1H), 3.95 (s, 3H), 3.87 (s, 3H), 3.83 (s, 3H), 3.80 (s, 3H), 1.45 (s, 9H). ¹³C NMR (101 MHz, CDCl₃): δ = 152.81, 149.71, 149.65, 146.41, 144.33, 139.13, 127.28, 119.17, 115.52, 113.38, 112.67, 98.61, 57.54, 56.51, 56.24, 55.67, 35.19, 29.65. HRMS (ESI): calcd. for C₂₀H₂₇O₅ (M+H)⁺, *m/z* 347.1853; found 347.1860.

3-(tert-Butyl)-2',4',5'-trimethoxy-[1,1'-biphenyl]-2,5-dione (4q): *R*_f = 0.33 (hexane/EtOAc, 3:1). ¹H NMR (300 MHz, CDCl₃): δ = 6.72 (s, 1H), 6.68 (d, *J* = 2.6 Hz, 1H), 6.60 (d, *J* = 2.6 Hz, 1H), 6.58 (s, 1H), 3.93 (s, 3H), 3.85 (s, 3H), 3.75 (s, 3H), 1.33 (s, 9H). ¹³C NMR (101 MHz, CDCl₃): δ = 188.32, 186.53, 157.18, 151.92, 151.43, 148.32, 143.26, 131.71, 130.99, 114.96, 113.61, 97.67, 56.60, 56.52, 56.15, 35.52, 29.24. HRMS (ESI): calcd. for C₁₉H₂₃O₅ (M+H)⁺, *m/z* 331.1540; found 331.1545.

1-(2-Hydroxy-3-methoxy-5-methylphenyl)-2-methoxynaphthalene (5ab):^[18a] ¹H NMR (300 MHz, CDCl₃): δ = 7.91 (d, *J* = 9.0 Hz, 1H), 7.85 – 7.81 (m, 1H), 7.52 – 7.46 (m, 1H), 7.40 (d, *J* = 9.0 Hz, 1H), 7.38 – 7.32 (m, 2H), 6.80 (d, *J* = 1.9 Hz, 1H), 6.67 (d, *J* = 2.0 Hz, 1H), 5.38 (s, 1H), 3.95 (s, 3H), 3.90 (s, 3H), 2.37 (s, 3H). ¹³C NMR (75 MHz, CDCl₃): δ = 154.21, 146.67, 141.29, 133.48, 129.52, 129.13, 128.86, 127.87, 126.37, 125.20, 124.31, 123.55, 122.09, 120.37, 113.82, 111.12, 56.92, 55.87, 21.22. MS (ESI): *m/z* (%) = 295.1 (100, MH⁺), 312.2 (34, MNH₂⁺), 611.2 (30, 2MNa⁺).

2-Hydroxy-2',3,4',6'-tetramethoxy-5-methyl-biphenyl (6ab):^[18a] ¹H NMR (300 MHz, CDCl₃): δ = 6.68 (d, *J* = 1.9 Hz, 1H), 6.60 (d, *J* = 1.8 Hz, 1H), 6.25 (s, 2H), 5.37 (s, 1H), 3.89 (s, 3H), 3.86 (s, 3H), 3.74 (s, 6H), 2.31 (s, 3H). ¹³C NMR (75 MHz, CDCl₃): δ = 160.98, 158.66, 146.59, 141.17, 128.33, 124.56, 120.34, 110.99, 107.34, 91.06, 56.06, 55.75, 55.34, 21.26. MS (ESI): *m/z* (%) = 305.1 (100, MH⁺), 631.3 (22, 2MNa⁺).

4-Hydroxy-2',3,4',5,6'-pentamethoxy-biphenyl (7ab):^[36d] *R*_f = 0.11 (hexane/EtOAc, 3:1). ¹H NMR (400 MHz, CDCl₃): δ = 6.57 (s, 2H), 6.23 (s, 2H), 5.50 (s, 1H), 3.87 (s, 6H), 3.87 (s, 3H), 3.74 (s, 6H). ¹³C NMR (101 MHz, CDCl₃): δ = 160.35, 158.41, 146.41, 133.50, 124.75, 112.46, 107.99, 90.95, 56.20, 55.93, 55.38. HRMS (ESI): calcd. for C₁₇H₂₁O₆ (M+H)⁺, *m/z* = 321.1333; found 321.1337.

2,3',4,5',6-Pentamethoxy-4'-(2,4,6-trimethoxyphenoxy)-1,1'-biphenyl (7abb):^[36d] *R*_f = 0.08 (hexane/EtOAc, 3:1). ¹H NMR (400 MHz, CDCl₃): δ = 6.53 (s, 2H), 6.21 (s, 2H), 6.15 (s, 2H), 3.85 (s, 3H), 3.77 (s, 3H), 3.72 (s, 6H), 3.70 (s, 6H), 3.69 (s, 6H). ¹³C NMR (101 MHz, CDCl₃): δ = 160.27, 158.40, 155.31, 152.29, 150.77, 136.45, 132.35, 127.88, 112.96, 109.72, 92.56, 91.33, 56.81, 56.66, 55.99, 55.42, 55.35. HRMS (ESI): calcd. for C₂₆H₃₁O₉ (M+H)⁺, *m/z* = 487.1963; found 487.1970.

4-Hydroxy-2',3,4',5,5'-pentamethoxy-biphenyl (9ab):^[18b] ¹H NMR (300 MHz, CDCl₃): δ = 6.86 (s, 1H), 6.73 (s, 2H), 6.62 (s, 1H), 5.61 (s, 1H), 3.92 (s, 3H), 3.90 (s, 3H), 3.89 (s, 3H), 3.87 (s, 3H), 3.76 (s, 3H). ¹³C

NMR (75 MHz, CDCl₃) δ = 150.51, 148.67, 146.53, 143.11, 133.68, 129.30, 122.45, 114.46, 106.25, 98.47, 56.70, 56.59, 56.20, 56.06. MS (ESI): *m/z* (%) = 321.1 (100, MH⁺), 663.2 (11, 2MNa⁺).

2,3',4,5,5'-Pentamethoxy-4'-(2,4,5-trimethoxyphenoxy)-1,1'-biphenyl (9abb): R_f = 0.29 (hexane/EtOAc, 1:1). ¹H NMR (400 MHz, 213 K, CDCl₃) δ = 6.90 (s, 1H), 6.78 – 6.74 (m, 2H), 6.62 (s, 1H), 6.61 (s, 1H), 6.24 (s, 1H), 3.99 (s, 3H), 3.95 (s, 3H), 3.94 (s, 3H), 3.89 (s, 3H), 3.85 (s, 3H), 3.79 (s, 6H), 3.66 (s, 3H). ¹³C NMR (101 MHz, 213 K, CDCl₃): δ = 152.32, 149.51, 147.94, 142.44, 141.82, 141.28, 140.87, 139.92, 135.08, 129.19, 120.19, 112.63, 105.35, 98.94, 97.01, 95.78, 56.72, 56.27, 56.07, 56.02, 55.99, 55.95, 55.88. HRMS (ESI): calcd. for C₂₆H₃₁O₉ (M+H)⁺, *m/z* = 487.1963; found 487.1966.

5-Ethyl-2-hydroxy-2',3,4',5'-tetramethoxybiphenyl (10ab): ¹H NMR (400 MHz, CDCl₃): δ = 6.87 (s, 1H), 6.74 (d, *J* = 2.0 Hz, 1H), 6.72 (d, *J* = 2.0 Hz, 1H), 6.66 (s, 1H), 5.97 (s, 1H), 3.94 (s, 3H), 3.92 (s, 3H), 3.86 (s, 3H), 3.81 (s, 3H), 2.64 (q, *J* = 7.6 Hz, 2H), 1.26 (t, *J* = 7.6 Hz, 3H). ¹³C NMR (101 MHz, CDCl₃): δ = 150.39, 149.26, 147.42, 143.57, 141.04, 135.69, 125.12, 122.20, 118.68, 115.12, 109.99, 98.48, 57.23, 56.47, 56.12, 55.99, 28.54, 15.71. HRMS (ESI): calcd. for C₁₈H₂₃O₅ (M+H)⁺, *m/z* = 319.1540; found 319.1546.

1-(4-Ethyl-2-methoxyphenoxy)-2,4,5-trimethoxybenzene (10ab'): ¹H NMR (400 MHz, CDCl₃): δ = 6.80 (d, *J* = 1.9 Hz, 1H), 6.64 (dd, *J* = 8.2, 1.9 Hz, 1H), 6.64 (s, 1H), 6.61 (s, 1H), 6.58 (d, *J* = 8.1 Hz, 1H), 3.91 (s, 3H), 3.89 (s, 3H), 3.80 (s, 3H), 3.74 (s, 3H), 2.61 (q, *J* = 7.6 Hz, 2H), 1.23 (t, *J* = 7.6 Hz, 3H). ¹³C NMR (101 MHz, CDCl₃): δ = 149.28, 145.63, 145.31, 145.03, 143.33, 138.90, 138.25, 119.59, 116.06, 112.08, 106.48, 100.41, 57.42, 56.54, 56.51, 55.97, 28.53, 15.66. HRMS (ESI): calcd. for C₁₈H₂₃O₅ (M+H)⁺, *m/z* = 319.1540; found 319.1549.

5-Ethyl-2',3,4',5'-tetramethoxy-2-(2,4,5-trimethoxyphenoxy)-1,1'-biphenyl (10abb): ¹H NMR (400 MHz, CDCl₃): δ = 6.81 – 6.79 (m, 2H), 6.78 (d, *J* = 2.0 Hz, 1H), 6.44 (s, 1H), 6.42 (s, 1H), 6.20 (s, 1H), 3.84 (s, 3H), 3.79 (s, 3H), 3.77 (s, 3H), 3.71 (s, 3H), 3.69 (s, 3H), 3.61 (s, 3H), 3.60 (s, 3H), 2.69 (q, *J* = 7.6 Hz, 2H), 1.28 (t, *J* = 7.6 Hz, 3H). ¹³C NMR (101 MHz, CDCl₃): δ = 152.30, 150.76, 148.61, 142.99, 142.76, 142.34, 142.24, 142.03, 140.46, 139.47, 132.49, 123.12, 118.10, 114.75, 111.04, 101.64, 100.99, 97.49, 57.44, 56.68, 56.65, 56.30, 56.07, 55.97, 55.92, 28.73, 15.30. HRMS (ESI): calcd. for C₂₇H₃₆O₈N (M+NH₄)⁺, *m/z* = 502.2435; found 502.2446.

5-Allyl-2-hydroxy-2',3,4',5'-tetramethoxybiphenyl (11ab): ¹H NMR (400 MHz, CDCl₃): δ = 6.86 (s, 1H), 6.73 – 6.69 (m, 2H), 6.65 (s, 1H), 6.06 – 5.94 (m, 2H), 5.16 – 5.04 (m, 2H), 3.94 (s, 3H), 3.91 (s, 3H), 3.86 (s, 3H), 3.80 (s, 3H), 3.37 (d, *J* = 6.8 Hz, 2H). ¹³C NMR (101 MHz, CDCl₃): δ = 150.41, 149.32, 147.53, 143.58, 141.43, 137.67, 131.46, 125.21, 123.05, 118.52, 115.63, 115.11, 110.52, 98.50, 57.26, 56.49, 56.13, 56.01, 39.94. HRMS (ESI): calcd. for C₁₉H₂₃O₅ (M+H)⁺, *m/z* = 331.1540; found 331.1545.

1-(4-Allyl-2-methoxyphenoxy)-2,4,5-trimethoxybenzene (11ab'): ¹H NMR (400 MHz, 213 K, CDCl₃): δ = 6.77 (d, *J* = 1.9 Hz, 1H), 6.69 (s, 1H), 6.64 – 6.56 (m, 2H), 6.43 (d, *J* = 8.2 Hz, 1H), 5.93 (ddt, *J* = 16.8, 10.0, 6.8 Hz, 1H), 5.15 – 5.01 (m, 2H), 3.94 (s, 3H), 3.93 (s, 3H), 3.79 (s, 3H), 3.76 (s, 3H), 3.34 (d, *J* = 6.8 Hz, 2H). ¹³C NMR (101 MHz, 213 K, CDCl₃): δ = 147.96, 145.45, 145.12, 144.73, 141.50, 137.38, 134.59, 133.64, 119.65, 115.90, 113.43, 111.22, 105.99, 96.63, 56.23, 55.92, 55.60, 39.75. HRMS (ESI): calcd. for C₁₉H₂₃O₅ (M+H)⁺, *m/z* = 331.1540; found 331.1547.

5-Allyl-2',3,4',5'-tetramethoxy-2-(2,4,5-trimethoxyphenoxy)-1,1'-biphenyl (11abb): ¹H NMR (400 MHz, CDCl₃): δ = 6.81 – 6.78 (m, 2H), 6.77 (d, *J* = 2.0 Hz, 1H), 6.44 (s, 1H), 6.42 (s, 1H), 6.19 (s, 1H), 6.03 (ddt, *J* = 16.7, 10.0, 6.6 Hz, 1H), 5.17 – 5.07 (m, 2H), 3.84 (s, 3H), 3.78 (s, 3H), 3.77 (s, 3H), 3.71 (s, 3H), 3.70 (s, 3H), 3.61 (s, 3H), 3.60 (s, 3H), 3.42 (d, *J* = 6.6 Hz, 2H). ¹³C NMR (101 MHz, CDCl₃): δ = 152.43, 150.76, 148.68, 143.04, 142.75, 142.35, 142.14, 142.04, 139.90, 137.28, 136.29, 132.62, 123.99, 117.91, 115.97, 114.72, 111.59, 101.60, 100.93, 97.46, 57.42, 56.66, 56.65, 56.30, 56.09, 55.99, 55.93, 40.10. HRMS (ESI): calcd. for C₂₈H₃₆O₈N (M+NH₄)⁺, *m/z* = 514.2435; found 514.2441.

2,2',4,4',5,5'-Hexamethoxy-1,1'-biphenyl (1bb):^[18a] ¹H NMR (300 MHz, CDCl₃): δ = 6.82 (s, 2H), 6.63 (s, 2H), 3.93 (s, 6H), 3.84 (s, 6H), 3.76 (s, 6H). ¹³C NMR (75 MHz, CDCl₃): δ = 151.16, 148.71, 142.79, 118.80, 115.17, 98.20, 56.81, 56.45, 56.02.

5-Chloro-2-hydroxy-2',3,4',5'-tetramethoxybiphenyl (12ab): ¹H NMR (400 MHz, CDCl₃): δ = 6.89 (d, *J* = 2.4 Hz, 1H), 6.86 (d, *J* = 2.4 Hz, 1H), 6.82 (s, 1H), 6.64 (s, 1H), 6.08 (s, 1H), 3.94 (s, 3H), 3.92 (s, 3H), 3.86 (s, 3H), 3.81 (s, 3H). ¹³C NMR (101 MHz, CDCl₃): δ = 150.35, 149.74, 148.15, 143.71, 141.96, 126.39, 124.46, 122.81, 117.11, 114.74, 110.69, 98.41, 57.29, 56.50, 56.27, 56.14. HRMS (ESI): calcd. for C₁₆H₁₈ClO₅ (M+H)⁺, *m/z* = 325.0837; found 325.0842.

1-(4-Chloro-2-methoxyphenoxy)-2,4,5-trimethoxybenzene (12ab'): ¹H NMR (400 MHz, CDCl₃): δ = 6.93 (d, *J* = 2.4 Hz, 1H), 6.77 (dd, *J* = 8.6, 2.4 Hz, 1H), 6.63 (s, 1H), 6.62 (s, 1H), 6.55 (d, *J* = 8.6 Hz, 1H), 3.90 (s, 3H), 3.89 (s, 3H), 3.77 (s, 3H), 3.76 (s, 3H). ¹³C NMR (101 MHz, CDCl₃): δ = 149.81, 146.40, 146.15, 145.01, 143.33, 137.12, 127.16, 120.29, 116.35, 112.73, 106.60, 100.09, 57.17, 56.51, 56.47, 56.16. HRMS (ESI): calcd. for C₁₆H₁₈ClO₅ (M+H)⁺, *m/z* = 325.0837; found 325.0839.

5-Chloro-2',3,4',5'-tetramethoxy-2-(2,4,5-trimethoxyphenoxy)-1,1'-biphenyl (12abb): ¹H NMR (400 MHz, CDCl₃): δ = 6.98 (d, *J* = 2.4 Hz, 1H), 6.93 (d, *J* = 2.4 Hz, 1H), 6.79 (s, 1H), 6.44 (s, 1H), 6.41 (s, 1H), 6.16 (s, 1H), 3.84 (s, 3H), 3.79 (s, 3H), 3.77 (s, 3H), 3.72 (s, 3H), 3.71 (s, 3H), 3.64 (s, 3H), 3.61 (s, 3H). ¹³C NMR (101 MHz, CDCl₃): δ = 153.16, 150.62, 149.12, 143.32, 142.68, 142.37, 142.04, 141.46, 140.59, 133.91, 129.38, 123.88, 116.30, 114.42, 111.75, 101.31, 100.59, 97.07, 57.26, 56.67, 56.57, 56.17, 56.11, 56.10, 55.98. HRMS (ESI): calcd. for C₂₅H₃₁ClO₈N (M+NH₄)⁺, *m/z* = 508.1733; found 508.1735.

3-Chloro-2-hydroxy-2',4',5'-trimethoxy-5-methyl-biphenyl (13ab):^[18b] ¹H NMR (300 MHz, CDCl₃): δ = 7.20 – 7.16 (m, 1H), 6.98 – 6.94 (m, 1H), 6.81 (s, 1H), 6.65 (s, 1H), 6.42 (s, 1H), 3.95 (s, 3H), 3.87 (s, 3H), 3.84 (s, 3H), 2.31 (s, 3H). ¹³C NMR (75 MHz, CDCl₃): δ = 149.79, 147.12, 144.03, 130.60, 130.23, 129.39, 127.05, 121.66, 117.89, 114.95, 98.19, 57.43, 56.51, 56.17, 20.41. MS (ESI): *m/z* (%) = 309.1 (100, MH⁺), 639.2 (7, 2MNa⁺).

1-(2-Chloro-4-methylphenoxy)-2,4,5-trimethoxybenzene (13ab'): ¹H NMR (400 MHz, CDCl₃): δ = 7.23 (d, *J* = 2.0 Hz, 1H), 6.90 (dd, *J* = 8.5, 2.1 Hz, 1H), 6.65 (s, 1H), 6.61 (s, 1H), 6.58 (d, *J* = 8.3 Hz, 1H), 3.89 (s, 3H), 3.79 (s, 3H), 3.77 (s, 3H), 2.28 (s, 3H). ¹³C NMR (101 MHz, CDCl₃): δ = 151.81, 146.19, 145.05, 143.55, 137.61, 132.69, 130.76, 128.07, 122.61, 116.32, 106.60, 100.75, 57.65, 56.53, 56.48, 20.36. HRMS (ESI): calcd. for C₁₆H₁₈ClO₄ (M+H)⁺, *m/z* = 309.0888; found 309.0887.

3'-Chloro-2,2'',4,4'',5,5''-hexamethoxy-5'-methyl-[1,1':4',1''-terphenyl]-2'-ol (13abb): Main regioisomer. ¹H NMR (300 MHz, CDCl₃): δ = 7.08 (s, 1H), 6.90 (s, 1H), 6.68 – 6.65 (m, 3H), 6.47 (s, 1H), 3.96 (s, 6H), 3.89 (s, 6H), 3.84 (s, 3H), 3.77 (s, 3H), 2.06 (s, 3H). ¹³C NMR (101 MHz, CDCl₃): δ = 150.83, 150.01, 149.71, 149.21, 147.35, 143.93, 143.15, 136.95,

130.25, 130.20, 125.49, 122.37, 119.14, 118.09, 115.21, 114.20, 98.15, 98.03, 57.31, 56.85, 56.56, 56.52, 56.20, 56.02, 20.05. HRMS (ESI): calcd. for $C_{25}H_{28}ClO_7$ (M+H)⁺, m/z = 475.1518; found 475.1527.

5'-(2,4,5-Trimethoxyphenyl)-[1,1':3',1"-terphenyl]-2'-ol (14ab): ¹H NMR (400 MHz, CDCl₃): δ = 7.64 – 7.59 (m, 4H), 7.53 – 7.47 (m, 4H), 7.47 (s, 2H), 7.43 – 7.37 (m, 2H), 6.93 (s, 1H), 6.64 (s, 1H), 5.43 (s, 1H), 3.94 (s, 3H), 3.87 (s, 3H), 3.81 (s, 3H). ¹³C NMR (101 MHz, CDCl₃): δ = 150.67, 148.80, 148.21, 143.33, 137.70, 130.90, 130.81, 129.44, 128.84, 128.41, 127.62, 121.67, 114.47, 98.29, 56.67, 56.65, 56.22. HRMS (ESI): calcd. for $C_{27}H_{25}O_4$ (M+H)⁺, m/z = 413.1747; found 413.1748.

2'-(2,4,5-Trimethoxyphenoxy)-1,1':3',1"-terphenyl (14ab'): ¹H NMR (400 MHz, CDCl₃): δ = 7.51 – 7.45 (m, 4H), 7.44 – 7.40 (m, 2H), 7.35 (dd, J = 8.5, 6.5 Hz, 1H), 7.31 – 7.24 (m, 4H), 7.24 – 7.18 (m, 2H), 6.29 (s, 1H), 6.01 (s, 1H), 3.70 (s, 3H), 3.60 (s, 3H), 3.52 (s, 3H). ¹³C NMR (101 MHz, CDCl₃): δ = 149.57, 143.18, 142.68, 142.14, 141.72, 137.92, 136.19, 130.60, 129.11, 127.83, 127.05, 125.21, 102.23, 100.92, 57.51, 56.66, 56.52. HRMS (ESI): calcd. for $C_{27}H_{25}O_4$ (M+H)⁺, m/z = 413.1747; found 413.1746.

2,4,5-Trimethoxy-5'-phenyl-4'-(2,4,5-trimethoxyphenoxy)-1,1':3',1"-terphenyl (14abb): ¹H NMR (400 MHz, 213 K, CDCl₃): δ = 7.66 (s, 2H), 7.55 – 7.46 (m, 4H), 7.36 – 7.28 (m, 4H), 7.28 – 7.21 (m, 2H), 6.96 (s, 1H), 6.64 (s, 1H), 6.31 (s, 1H), 6.17 (s, 1H), 4.01 (s, 3H), 3.92 (s, 3H), 3.86 (s, 3H), 3.77 (s, 3H), 3.69 (s, 3H), 3.60 (s, 3H). ¹³C NMR (101 MHz, 213 K, CDCl₃): δ = 149.52, 147.90, 147.50, 141.93, 141.14, 140.96, 140.22, 137.47, 135.11, 134.68, 131.42, 128.81, 127.77, 126.97, 118.90, 112.57, 100.20, 97.39, 95.51, 56.64, 56.30, 55.97, 55.87, 55.84, 55.74. HRMS (ESI): calcd. for $C_{36}H_{38}O_7N$ (M+NH₄)⁺, m/z = 596.2643; found 596.2646.

X-ray Crystallographic Details for Compounds 2q and 3q: CCDC 1510097 (for **2q**) and 1510098 (for **3q**) provide the supplementary crystallographic data for this paper. These data can be obtained free of charge from The Cambridge Crystallographic Data Centre.

Supporting Information (see footnote on the first page of this article): ¹H and ¹³C NMR spectra, cyclic voltammograms, mass spectra, crystallographic data and structures of compounds **2q** and **3q**, comprehensive optimization study, mechanistic investigations and reaction profiles.

Acknowledgements

This work was financially supported by the German Science Foundation (DFG) (GRK 1626, Chemical Photocatalysis). A. E. thanks the Deutsche Bundesstiftung Umwelt (DBU) for a graduate scholarship. We thank Dr. Rudolf Vasold (University of Regensburg) for his assistance in LC and GC-MS measurements, Regina Hoheisel (University of Regensburg) for her assistance in CV measurements.

Keywords: cross-dehydrogenative coupling • photocatalysis • phenols • biaryls • C–O coupling

[1] a) G. Bringmann, T. Gulder, T. A. M. Gulder, M. Breuning, *Chem. Rev.* **2011**, *111*, 563-639; b) G. Bringmann, A. J. Price Mortimer, P. A. Keller, M. J. Gresser, J. Garner, M. Breuning, *Angew. Chem. Int. Ed.* **2005**, *44*, 5384-5427; c) G. Bringmann, R. Walter, R. Weirich, *Angew. Chem. Int.*

- Ed. Engl.* **1990**, *29*, 977-991; d) W. Schuehly, Juan Manuel V. Paredes, J. Kleyer, A. Huefner, S. Anavi-Goffer, S. Raduner, K.-H. Altmann, J. Gertsch, *Chem. Biol.* **2011**, *18*, 1053-1064; e) M. C. Kozlowski, B. J. Morgan, E. C. Linton, *Chem. Soc. Rev.* **2009**, *38*, 3193-3207; f) P. Lloyd-Williams, E. Giralt, *Chem. Soc. Rev.* **2001**, *30*, 145-157; g) A. V. R. Rao, M. K. Gurjar, K. L. Reddy, A. S. Rao, *Chem. Rev.* **1995**, *95*, 2135-2167; h) J. Yamaguchi, A. D. Yamaguchi, K. Itami, *Angew. Chem. Int. Ed.* **2012**, *51*, 8960-9009.
- [2] a) J. Ralph, K. Lundquist, G. Brunow, F. Lu, H. Kim, P. F. Schatz, J. M. Marita, R. D. Hatfield, S. A. Ralph, J. H. Christensen, W. Boerjan, *Phytochem. Rev.* **2004**, *3*, 29-60; b) N. Geib, K. Woithe, K. Zerbe, D. B. Li, J. A. Robinson, *Bioorg. Med. Chem. Lett.* **2008**, *18*, 3081-3084; c) G. Brunow, I. Kilpeläinen, J. Sipilä, K. Syrjänen, P. Karhunen, H. Setälä, P. Rummakko, in *Lignin and Lignan Biosynthesis*, Vol. 697, American Chemical Society, **1998**, pp. 131-147.
- [3] a) J. M. Brunel, *Chem. Rev.* **2005**, *105*, 857-898; b) P. W. N. M. v. Leeuwen, P. C. J. Kamer, C. Claver, O. Pàmies, M. Diéguez, *Chem. Rev.* **2011**, *111*, 2077-2118; c) P. Kočovský, Š. Vyskočil, M. Smrčina, *Chem. Rev.* **2003**, *103*, 3213-3246; d) D. Parmar, E. Sugiono, S. Raja, M. Rueping, *Chem. Rev.* **2014**, *114*, 9047-9153.
- [4] a) A. C. Grimsdale, K. Leok Chan, R. E. Martin, P. G. Jokisz, A. B. Holmes, *Chem. Rev.* **2009**, *109*, 897-1091; b) L. Pu, *Chem. Rev.* **1998**, *98*, 2405-2494; c) S.-J. Su, D. Tanaka, Y.-J. Li, H. Sasabe, T. Takeda, J. Kido, *Org. Lett.* **2008**, *10*, 941-944; d) P. Kirsch, M. Bremer, *Angew. Chem.* **2000**, *39*, 4216-4235.
- [5] a) N. Miyaura, A. Suzuki, *Chem. Rev.* **1995**, *95*, 2457-2483; b) E.-i. Negishi, *Handbook of Organopalladium Chemistry for Organic synthesis*, **2002**; c) J. Hassan, M. Sévignon, C. Gozzi, E. Schulz, M. Lemaire, *Chem. Rev.* **2002**, *102*, 1359-1470; d) J. Magano, J. R. Dunetz, *Chem. Rev.* **2011**, *111*, 2177-2250; e) K. C. Nicolaou, P. G. Bulger, D. Sarlah, *Angew. Chem. Int. Ed.* **2005**, *44*, 4442-4489; f) V. Farina, V. Krishnamurthy, W. J. Scott, in *Organic Reactions*, John Wiley & Sons, Inc., **2004**; g) A. de Meijere, F. Diederich, *Metal-catalyzed Cross-coupling Reactions*, **2004**.
- [6] a) T. W. Lyons, M. S. Sanford, *Chem. Rev.* **2010**, *110*, 1147-1169; b) D. Alberico, M. E. Scott, M. Lautens, *Chem. Rev.* **2007**, *107*, 174-238; c) G. P. McGlacken, L. M. Bateman, *Chem. Soc. Rev.* **2009**, *38*, 2447; d) I. Hussain, T. Singh, *Adv. Synth. Catal.* **2014**, *356*, 1661-1696; e) X. Chen, K. M. Engle, D.-H. Wang, J.-Q. Yu, *Angew. Chem. Int. Ed.* **2009**, *48*, 5094-5115; f) L. Ackermann, R. n. Vicente, A. R. Kapdi, *Angew. Chem. Int. Ed.* **2009**, *48*, 9792-9826.
- [7] a) D. P. Hari, P. Schroll, B. König, *J. Am. Chem. Soc.* **2012**, *134*, 2958-2961; b) I. Ghosh, T. Ghosh, J. I. Bardagi, B. König, *Science* **2014**, *346*, 725-728; c) I. Ghosh, B. König, *Angew. Chem. Int. Ed.* **2016**, *55*, 7676-7679; d) R. B. Bedford, S. J. Coles, M. B. Hursthouse, M. E. Limmert, *Angew. Chem. Int. Ed.* **2003**, *42*, 112-114; e) R. B. Bedford, M. E. Limmert, *J. Org. Chem.* **2003**, *68*, 8669-8682; f) S. Oi, S.-i. Watanabe, S. Fukita, Y. Inoue, *Tetrahedron Lett.* **2003**, *44*, 8665-8668; g) C.-L. Ciana, R. J. Phipps, J. R. Brandt, F.-M. Meyer, M. J. Gaunt, *Angew. Chem. Int. Ed.* **2011**, *50*, 458-462; h) T. Satoh, M. Miura, *J. Synth. Org. Chem. Jpn.* **2006**, *64*, 1199-1207.
- [8] a) J. A. Ashenhurst, *Chem. Soc. Rev.* **2010**, *39*, 540-548; b) C. S. Yeung, V. M. Dong, *Chem. Rev.* **2011**, *111*, 1215-1292; c) A. A. O. Sarhan, C. Bolm, *Chem. Soc. Rev.* **2009**, *38*, 2730.
- [9] a) D. R. Stuart, K. Fagnou, *Science* **2007**, *316*, 1172-1175; b) D. R. Stuart, E. Villemure, K. Fagnou, *J. Am. Chem. Soc.* **2007**, *129*, 12072-12073.
- [10] a) M. Hovorka, J. Günterová, J. í. Závada, *Tetrahedron Lett.* **1990**, *31*, 413-416; b) M. Hovorka, R. Ščigel, J. Gunterová, M. Tichý, J. Závada, *Tetrahedron* **1992**, *48*, 9503-9516; c) M. Hovorka, J. Závada, *Tetrahedron* **1992**, *48*, 9517-9530; d) M. Smrčina, J. Polakova, S. Vyskočil, P. Kočovský, *J. Org. Chem.* **1993**, *58*, 4534-4538; e) M. Smrčina, S. Vyskočil, B. Máca, M. Polášek, T. A. Claxton, A. P. Abbott, P. Kočovský, *J. Org. Chem.* **1994**, *59*, 2156-2163.

- [11] a) K. Ding, W. Yang, L. Zhang, W. Yangjie, T. Matsuura, *Tetrahedron* **1996**, *52*, 1005-1010; b) F. Toda, K. Tanaka, S. Iwata, *J. Org. Chem.* **1989**, *54*, 3007-3009.
- [12] J. Doussot, A. Guy, C. Ferroud, *Tetrahedron Lett.* **2000**, *41*, 2545-2547.
- [13] G. Sartori, R. Maggi, F. Bigi, M. Grandi, *J. Org. Chem.* **1993**, *58*, 7271-7273.
- [14] S. R. Waldvogel, E. Aits, C. Holst, R. Fröhlich, *Chem. Commun.* **2002**, 1278-1279.
- [15] A. McKillop, A. G. Turrell, D. W. Young, E. C. Taylor, *J. Am. Chem. Soc.* **1980**, *102*, 6504-6512.
- [16] a) H. Egami, K. Matsumoto, T. Oguma, T. Kunisu, T. Katsuki, *J. Am. Chem. Soc.* **2010**, *132*, 13633-13635; b) Y. E. Lee, T. Cao, C. Torruellas, M. C. Kozłowski, *J. Am. Chem. Soc.* **2014**, *136*, 6782-6785; c) Q.-X. Guo, Z.-J. Wu, Z.-B. Luo, Q.-Z. Liu, J.-L. Ye, S.-W. Luo, L.-F. Cun, L.-Z. Gong, *J. Am. Chem. Soc.* **2007**, *129*, 13927-13938; d) S.-W. Hon, C.-H. Li, J.-H. Kuo, N. B. Barhate, Y.-H. Liu, Y. Wang, C.-T. Chen, *Org. Lett.* **2001**, *3*, 869-872; e) T. Temma, B. Hatano, S. Habauae, *Tetrahedron* **2006**, *62*, 8559-8563; f) R. Li, L. Jiang, W. Lu, *Organometallics* **2006**, *25*, 5973-5975.
- [17] a) T. Dohi, T. Kamitanaka, S. Watanabe, Y. Hu, N. Washimi, Y. Kita, *Chem. Eur. J.* **2012**, *18*, 13614-13618; b) K. Morimoto, K. Sakamoto, Y. Ohnishi, T. Miyamoto, M. Ito, T. Dohi, Y. Kita, *Chem. Eur. J.* **2013**, *19*, 8726-8731; c) Y. Kita, T. Dohi, *Chem. Rec.* **2015**, *15*, 886-906; d) K. Morimoto, K. Sakamoto, T. Ohshika, T. Dohi, Y. Kita, *Angew. Chem. Int. Ed.* **2016**, *55*, 3652-3656.
- [18] a) A. Kirste, G. Schnakenburg, F. Stecker, A. Fischer, S. R. Waldvogel, *Angew. Chem. Int. Ed.* **2010**, *49*, 971-975; b) A. Kirste, B. Elsler, G. Schnakenburg, S. R. Waldvogel, *J. Am. Chem. Soc.* **2012**, *134*, 3571-3576; c) B. Elsler, D. Schollmeyer, K. M. Dyballa, R. Franke, S. R. Waldvogel, *Angew. Chem. Int. Ed.* **2014**, *53*, 5210-5213; d) B. Elsler, A. Wiebe, D. Schollmeyer, K. M. Dyballa, R. Franke, S. R. Waldvogel, *Chem. Eur. J.* **2015**, *21*, 12321-12325.
- [19] a) E. Gaster, Y. Vainer, A. Regev, S. Narute, K. Sudheendran, A. Werbeloff, H. Shalit, D. Pappo, *Angew. Chem. Int. Ed.* **2015**, *54*, 4198-4202; b) A. Libman, H. Shalit, Y. Vainer, S. Narute, S. Kozuch, D. Pappo, *J. Am. Chem. Soc.* **2015**, *137*, 11453-11460.
- [20] T. Kashiwagi, B. Elsler, S. R. Waldvogel, T. Fuchigami, M. Atobe, *J. Electrochem. Soc.* **2013**, *160*, G3058-G3061.
- [21] The concept of Pappo *et al.*^[19b] based on early work of Kočovský and coworker^[10a].
- [22] Selected reviews and books: a) F. Teplý, *Collect. Czech. Chem. Commun.* **2011**, *76*, 859-917; b) B. König, *Chemical Photocatalysis*, De Gruyter, **2013**; c) C. K. Priier, D. A. Rankic, D. W. C. MacMillan, *Chem. Rev.* **2013**, *113*, 5322-5363.
- [23] T. Hamada, H. Ishida, S. Usui, Y. Watanabe, K. Tsumura, K. Ohkubo, *J. Chem. Soc., Chem. Commun.* **1993**, 909-911.
- [24] a) T. R. Blum, Y. Zhu, S. A. Nordeen, T. P. Yoon, *Angew. Chem. Int. Ed.* **2014**, *53*, 11056-11059; b) T. Song, B. Zhou, G.-W. Peng, Q.-B. Zhang, L.-Z. Wu, Q. Liu, Y. Wang, *Chem. Eur. J.* **2014**, *20*, 678-682.
- [25] D. C. Fabry, M. A. Ronge, J. Zoller, M. Rueping, *Angew. Chem. Int. Ed.* **2015**, *54*, 2801-2805.
- [26] a) M. Haga, E. S. Dodsworth, G. Eryavec, P. Seymour, A. B. P. Lever, *Inorg. Chem.* **1985**, *24*, 1901-1906; b) C. R. Bock, J. A. Connor, A. R. Gutierrez, T. J. Meyer, D. G. Whitten, B. P. Sullivan, J. K. Nagle, *J. Am. Chem. Soc.* **1979**, *101*, 4815-4824.
- [27] Y. Zhao, B. Huang, C. Yang, W. Xia, *Org. Lett.* **2016**, *18*, 3326-3329.
- [28] N. A. Romero, K. A. Margrey, N. E. Tay, D. A. Nicewicz, *Science* **2015**, *349*, 1326-1330.
- [29] C. Bronner, O. S. Wenger, *J. Phys. Chem. Lett.* **2012**, *3*, 70-74.
- [30] S. K. Reddy Parumala, R. K. Peddinti, *Org. Lett.* **2013**, *15*, 3546-3549.
- [31] a) S. Yamazaki-Nishida, M. Kimura, *Bull. Chem. Soc. Jpn.* **1991**, *64*, 1840-1845; b) H. S. White, W. G. Becker, A. J. Bard, *J. Phys. Chem.* **1984**, *88*, 1840-1846; c) A. Lewandowska-Andralojc, D. E. Polyansky, *J. Phys. Chem. A* **2013**, *117*, 10311-10319; d) F. Bolletta, A. Juris, M. Maestri, D. Sandrini, *Inorg. Chim. Acta* **1980**, *44*, L175-L176.
- [32] For the comprehensive optimization study see Table S1 and Table S2 in the SI.
- [33] The cross-dehydrogenative C–O bond formation between anilines and phenols was published during the revision of this manuscript: C. Heitz, A. W. Jones, B. S. Oezkaya, C. L. Bub, M.-L. Louillat-Habermeyer, V. Wagner, F. W. Patureau, *Chem. Eur. J.* **2016**, *22*, 17980-17982.
- [34] Roy *et al.* demonstrated, that the relative nucleophilicity of phenols and arenes correlates to the energy of their highest occupied molecular orbital (HOMO), which can be easily accessed by DFT methods: S. Pratihari, S. Roy, *J. Org. Chem.* **2010**, *75*, 4957-4963.
- [35] S. Grimme, J. Antony, S. Ehrlich, H. Krieg, *J. Chem. Phys.* **2010**, *132*, 154104.
- [36] a) K. M. Johnston, R. E. Jacobson, G. H. Williams, *J. Chem. Soc. C* **1969**, 1424-1427; b) T. J. Stone, W. A. Waters, *J. Chem. Soc.* **1964**, 213-218; c) J. R. J. Fehir, J. K. McCusker, *J. Phys. Chem. A* **2009**, *113*, 9249-9260; d) A. Dyadyuk, K. Sudheendran, Y. Vainer, V. Vershinin, A. I. Shames, D. Pappo, *Org. Lett.* **2016**, *18*, 4324-4327; e) M. Lucarini, V. Mugnaini, G. F. Pedulli, M. Guerra, *J. Am. Chem. Soc.* **2003**, *125*, 8318-8329; f) In most of our systems the *para* or *ortho* position is blocked by a substituent, therefore in this study *ortho/para* regioselectivity is not relevant; g) W. A. Yehye, N. A. Rahman, A. Ariffin, S. B. Abd Hamid, A. A. Alhadi, F. A. Kadir, M. Yaeghoobi, *Eur. J. Med. Chem.* **2015**, *101*, 295-312.
- [37] Literature for the electrophilic nature of phenoxyl radicals: a) F. D. Vleeschouwer, V. V. Speybroeck, M. Waroquier, P. Geerlings, F. D. Proft, *The Journal of Organic Chemistry* **2008**, *73*, 9109-9120; b) F. De Vleeschouwer, V. Van Speybroeck, M. Waroquier, P. Geerlings, F. De Proft, *Org. Lett.* **2007**, *9*, 2721-2724.
- [38] a) Y.-D. Wu, D. K. W. Lai, *J. Org. Chem.* **1996**, *61*, 7904-7910; b) C. Aliaga, I. Almodovar, M. C. Rezende, *J. Mol. Model.* **2015**, *21*, 1-10.
- [39] V. V. Pavlishchuk, A. W. Addison, *Inorg. Chim. Acta* **2000**, *298*, 97-102.
- [40] In case of the *ortho*-alkoxyphenols the corresponding 1,2-benzoquinone coupling products were not observed as by-products.
- [41] Yoon and coworkers^[24a] postulated a slow salt metathesis, which provide the Ru(bpz)₃(S₂O₈) as active catalyst after an induction period. We could confirm the observations and a similar induction period was detected (see SI).
- [42] a) F. Minisci, A. Citterio, C. Giordano, *Acc. Chem. Res.* **1983**, *16*, 27-32; b) R. E. Huie, C. L. Clifton, P. Neta, *Radiat. Phys. Chem.; Int. J. Radiat. Appl. Instrum., Part C* **1991**, *38*, 477-481.
- [43] Persulfate salts are reported in some cases as direct oxidant for phenolic systems at elevated temperatures or under irradiation: e.g. ref [27] and a) W. Xia, Y. Zhao, B. Huang, C. Yang, B. Li, *Synthesis* **2015**, *47*, 2731-2737. Control experiments exclude ammonium persulfate as efficient oxidant, see Table 1. However, the SO₄^{•-} formed after oxidative quenching is a strong oxidant and can in principle be involved in the phenol oxidation. Jeganmohan *et al.* reported a method for the oxidative cross-coupling of phenols using K₂S₂O₈ and Bu₄N⁺·HSO₃⁻ (10 mol%) in CF₃COOH. However, the method is restricted to strongly acidic media: b) N. Y. More, M. Jeganmohan, *Org. Lett.* **2015**, *17*, 3042-3045.
- [44] Trace amounts of the homocoupling product of **5a** were detected by mass analysis for entry 7.
- [45] L. Biczók, N. Gupta, H. Linschitz, *J. Am. Chem. Soc.* **1997**, *119*, 12601-12609.
- [46] The DFT calculations of the nucleophilicity *N* values do not consider solvent or hydrogen bonding effects. The true nucleophilicity of the phenols (*O*-nucleophile) compared to the arene components may differ, but within the substance class **a** the values are comparable.
- [47] The purification and isolation of the cross-coupling products (**1ab**, **1ab'** and **1abb**) could be achieved easily, despite their similar structures, by column chromatography (see Figure S14 in SI).
- [48] Waldvogel *et al.* reported very recently a selective electrochemical strategy for the synthesis of *meta*-terphenyl-2,2"-diols: S. Lips, A. Wiebe, B. Elsler, D. Schollmeyer, K. M. Dyballa, R. Franke und S. R.

Waldvogel, *Angew. Chem. Int. Ed.* **2016**, *55*, 10872-10876. Pappo *et al.*^[36d] developed very recently a method for the consecutive formation of teraryls.

- [49] a) J. F. Hartwig, *Angew. Chem. Int. Ed.* **1998**, *37*, 2046-2067; b) J. Scott Sawyer, *Tetrahedron* **2000**, *56*, 5045-5065; c) S. V. Ley, A. W. Thomas, *Angew. Chem. Int. Ed.* **2003**, *42*, 5400-5449; d) D. Kikelj, R. Frlan, *Synthesis* **2006**, *2006*, 2271-2285; e) F. Monnier, M. Taillefer, *Angew. Chem. Int. Ed.* **2009**, *48*, 6954-6971; f) N. Jalalian, T. B. Petersen, B. Olofsson, *Chem. Eur. J.* **2012**, *18*, 14140-14149; g) V. P. Mehta, B. Punji, *RSC Adv.* **2013**, *3*, 11957; h) A. S. Hay, *J. Polym. Sci., Part A: Polym. Chem.* **1998**, *36*, 505-517.
- [50] Z. Liu, Y. Zhao, Y. Zhang, J. Wang, H. Li, L. Wu, *Synlett* **2010**, *2010*, 2352-2356.

WILEY-VCH

Accepted Manuscript

FULL PAPER

No leaving groups required – C–C vs C–O cross-coupling driven by visible light. Formation of C–C and C–O cross-coupling products of phenol and arenes by direct C–H activation was accomplished by visible light photoredox catalysis. The efficiency and chemoselectivity (homo- vs. cross-coupling and C–C vs. C–O) were rationalized on basis of the oxidation potentials E_{ox} and nucleophilicity N values of the aromatic substrates.

**Photoredox catalysis***

Author(s), Corresponding Author(s)*

Page No. – Page No.**Title**